# Noise-Induced Stabilization in Population Dynamics

Matthew Parker, Alex Kamenev, and Baruch Meerson

Phys. Rev. Lett. **107**, 180603 — Published 27 October 2011

DOI: 10.1103/PhysRevLett.107.180603

# Noise induced stabilization in population dynamics

Matthew Parker,[1] Alex Kamenev,[1,2] and Baruch Meerson[3]

[1] *School of Physics and Astronomy, University of Minnesota, Minneapolis, MN 55455*
[2] *William I. Fine Theoretical Physics Institute, University of Minnesota, Minneapolis, MN 55455*
[3] *Racah Institute of Physics, Hebrew University of Jerusalem, Jerusalem 91904, Israel*

We investigate a model where strong noise in a sub-population creates a metastable state in an otherwise unstable two-population system. The induced metastable state is vortex-like, and its persistence time grows exponentially with the noise strength. A variety of distinct scaling relations are observed depending on the relative strength of the sub-population noises.

The phenomenon of noise induced metastability [1–3] is of importance in ecology [4] and plant biology [5] and has found practical applications in engineering [6]. The typical models [1–3] consider periodically modulated one-dimensional (1d) stochastic systems. The modulation renders the system deterministically unstable during a part of the modulation period. An external noise can prevent the escape for several successive periods of external modulation, trapping the system into a metastable state. As a result, the noise may cause an increase of the mean persistence time by a factor of (about) two [1].

Here we consider a different model with two stochastic degrees of freedom, which we call $x$ and $y$. The $y$ degree of freedom (e.g. imbalance between the numbers of two competing gene alleles) undergoes a strong and fast fluctuations which conserve the total population size $x$. The latter experiences a slow evolution under the influence of a deterministic potential $V(x)$ along with a sign-definite feedback from the population size imbalance $\propto y^2$ and a relatively weak (demographic) noise. We show that, even if the $x$-dynamics itself is unstable and prone to a rapid escape, the strong $y$-noise can lock it in an *exponentially* long-lived vortex-like metastable state. The corresponding exponent exhibits a variety of non-trivial scaling regimes, depending on the relative strength of the noises in the $x$ and $y$ subsystems. A similar model was shown to describe a two-patch Lotka-Volterra system [7]. More distantly related models were recently discussed in the context of biochemical regulatory networks [8] and nanomechanical oscillators [9].

Our model can be cast into the universal form

$$\begin{aligned} &\dot{x} = -V'(x) - y^2 + \xi_x(t)\,, \\ &\dot{y} = -2y + \xi_y(t)\,; \\ &\langle \xi_{x(y)}(t)\xi_{x(y)}(t')\rangle = 2T_{x(y)}\delta(t-t')\,, \end{aligned} \tag{1}$$

where $V' = dV(x)/dx$, and $T_x$ and $T_y$ characterize the noise strength in the total and differential population size, respectively. The interesting regime of parameters is $T_x < T_y$. The noise effects are substantial when the population is close to a saddle point. In this case the properly rescaled deterministic potential takes the form

$$V(x) = -x^3/3 - \epsilon x, \tag{2}$$

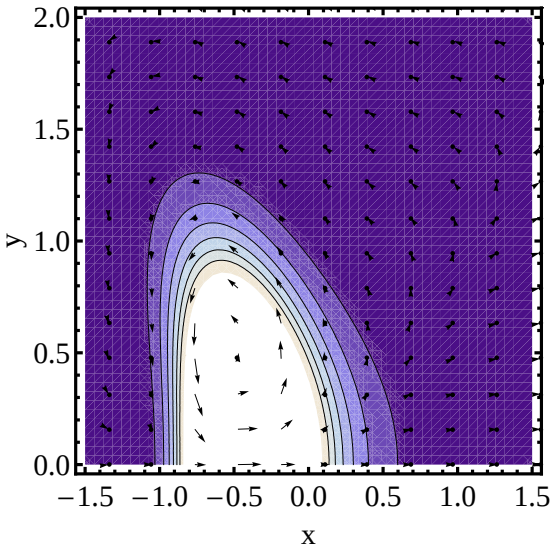


FIG. 1. (Color online) The quasi-stationary FP state. The contours represent the probability density $P(x,y)$; the arrows show the probability current density. The system is symmetric around $y = 0$, and only the top half is shown. $T_x = 0.05, T_y = 0.5$.

where $\epsilon$ is the bifurcation parameter, and we have shifted the $x$ variable to have the bifurcation point at $x = 0$. In this form, $\epsilon > 0$ corresponds to a system that is unstable in the $x$-direction, and $\epsilon < 0$ represents a stable system.

A simple realization of this model is provided by two species $A$ and $B$, which undergo the reaction $A + B \xrightarrow{\lambda} 2X$, where $X$ is either $A$ or $B$. This is the well-known Moran process for modeling neutral genetic drift [10] where $A$ and $B$ represent two equally fit alleles. This is the fastest reaction which conserves the total population size. In addition, the total population size may slowly evolve according to e.g. the following set of reactions $X \overset{\beta_\mp}{\leftrightarrow} 0$ and $A + B \xrightarrow{\alpha} A + B + X$. In this case $x = (n_A + n_B - N)/N$ and $y = (n_A - n_B)/N$, where $N = \beta_-/\alpha$ is the population size close to the bifurcation, and $\epsilon = 4\alpha\beta_+/\beta_-^2 - 1$ is the bifurcation parameter. Under this reaction scheme both species are equally fit, however, certain configurations ($n_A \approx n_B$) favor a larger

total population size. In the limit of large population size $N \gg 1$, the corresponding Master equation can be approximated by a Fokker-Planck equation [11]. In the vicinity of the bifurcation point, the latter reads

$$\dot{P}(x,y) = -\partial_x\left[\left(-V'(x)-y^2\right)P(x,y) - \frac{2}{N}\partial_x P(x,y)\right] - \partial_y\left[-2yP(x,y) - \left(\lambda+\frac{2}{N}\right)\partial_y P(x,y)\right], \quad (3)$$

where $P(x,y,t)$ is the probability distribution function, and time is measured in units of $2/\beta_-$. Equation (3) is equivalent to the Langevin equations (1), where the two "temperatures" are given by $T_x = 2/N$ and $T_y = T_x + 2\lambda/\beta_-$. When the drift rate $\lambda$ is fast, one has the strong inequality $T_x \ll T_y$.

First we focus on the system exactly at bifurcation, $\epsilon = 0$. The $x$-equation takes the form $\dot{x} = x^2 - y^2 + \xi_x$. Without noise the $y$-variable tends to zero, leading to $\dot{x} = x^2$ dynamics in the $x$-direction. This has $x = 0$ as the nonlinearly unstable point. An arbitrarily weak $x$-noise is sufficient to kick the system out of this fixed point and set it on the path to unlimited proliferation, $x \to \infty$. One may think thus that the $\epsilon = 0$ system is destined to blow up in a very short time. Recall, however, that the $y$-noise is substantial. Although $\langle y\rangle = 0$, the mean square value $\langle y^2\rangle > 0$ and is large compared with $T_x$. One can then expect the $x$-dynamics to be governed by the effective potential $V_{\rm eff}(x) = -x^3/3 + \langle y^2\rangle x$. This potential exhibits a minimum at $x = -\sqrt{\langle y^2\rangle}$, and a maximum at $x = \sqrt{\langle y^2\rangle}$. As a result, a long-lived metastable distribution, peaked at $x = -\sqrt{\langle y^2\rangle}$, can be created. A numerical solution of the Fokker-Planck (FP) equation (3) supports this expectation. Figure 1 shows the slowly varying quasi-stationary distribution observed at late times. Notably, the probability currents develop two counter-rotating vortices. Before reaching the point $x = y = 0$, the "particle" is kicked in the $y$-direction, where the $x$-evolution is directed toward population contraction. Instead of immediately undergoing a population explosion, the system is trapped in this vortex state. We note that probability current vortices in non-equilibrium *stationary* states – the Brownian vortices – were recently observed in experiment [12].

Our main goal is to evaluate the lifetime of such a noise-induced vortex-like metastable state. We start from qualitative considerations. As a first approximation one can estimate the mean-square $y$-deviation in the harmonic potential $y^2$, cf. Eq. (1), as $\langle y^2\rangle = T_y/2$. The effective 1d potential height (in the $x$-direction) is therefore $V_{\rm eff}^{\max} - V_{\rm eff}^{\min} = \sqrt{2}\,T_y^{3/2}/3$, and one expects that

$$\ln t_{\rm esc} \simeq \sqrt{2}\,T_y^{3/2}/3T_x\,. \quad (4)$$

Remarkably, the escape time is exponentially *increasing* with the $y$-noise strength $T_y$, while exhibiting the standard Arrhenius scaling with $T_x$. Our numerical simulations of the Langevin Eqs. (1), see Fig. 2, confirm Eq. (4) as long as $T_y^{3/2}/T_x$ is not too large. At larger values of this parameter, however, Eq. (4) greatly overestimates the lifetime of the metastable state.

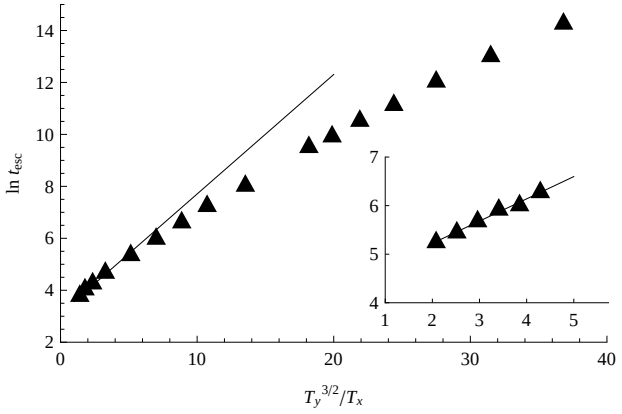


FIG. 2. Simulated escape times for $T_y = 0.05$ and varying $T_x$ ($\epsilon = 0$). The straight line has slope of $\sqrt{2}/3$, cf. Eq. (4). Inset: the limit $\sqrt{T_x} > T_y$.

The reason for this deviation is that for large $T_y$ the typical potential barrier is too high for the $x$-motion to overcome. Then, instead of relying on typical realizations of $y$-noise, it is more likely that the system waits for a rare $y$-trajectory which stays anomalously close to $y = 0$. The probability that the $y$-motion is confined to the interval $|y(t)| < y_0$ for a time $t_0$ is given by $\exp[-E_y(y_0)t_0]$. Here $E_y$ is the lowest eigenvalue of the 1d FP equation in the $y$-direction with absorbing boundary conditions at $y = \pm y_0$. It can be estimated as $E_y \propto T_y/y_0^2$, where $T_y$ is the $y$-diffusion coefficient. On the other hand, the probability that during the time interval $t_0$ the $x$-coordinate will diffuse from $x = -y_0$ to $x = +y_0$ is given by $\exp(-y_0^2/T_x t_0)$, where $T_x$ is the diffusion coefficient in the $x$-direction. Maximizing the product of these two probabilities with respect to $y_0^2/t_0$, one finds that the probability of the optimal rare fluctuation scales as $\exp(-\sqrt{T_y/T_x})$. These estimates suggest that $\ln t_{\rm esc} \propto \sqrt{T_y/T_x}$ once $\sqrt{T_y/T_x} < T_y^{3/2}/T_x$, i.e. $\sqrt{T_x} < T_y$. This behavior is indeed qualitatively consistent with Fig. 2.

To put these considerations on a more quantitative basis we shall assume that the dynamics can be separated into the fast $y$-motion and slow $x$-motion. The latter adiabatically adjusts to the instantaneous value of $y^2(t)$. We then solve an auxiliary problem of finding the probability of $y$-trajectories with a given functional form $\langle y^2\rangle = y_0^2(t)$. Here $y_0(t)$ is an arbitrary *slow* function of time, such that $y_0(\pm\infty) = \sqrt{T_y/2}$, while the averaging is taken over the fast $y$-fluctuations. In the rescaled units, the fast time scale is taken to be unity, cf. Eq. (1). The

function $y_0(t)$ then evolves on a time scale parametrically larger than this and determined by the parameter $T_y/T_x^{1/2}$. Integrating over an intermediate time-scale $\Delta t$ that is long relative to the fast fluctuations one can then write $\int_{t-\Delta t}^{t+\Delta t}[y_0^2(t) - y^2(t)]dt = 0$. We can thus introduce the functional constraint $\delta\big(\int[y^2(t) - y_0^2(t)]dt\big)$ into the stochastic functional integral over $\mathcal{D}y$ [13–16] and elevate it into the exponent with the help of the auxiliary *slow* field $\chi(t)$. As a result we obtain an effective Lagrangian

$$\mathcal{L}_y = \frac{(\dot{y} + 2y)^2}{4T_y} - \chi(y_0^2 - y^2)\,, \tag{5}$$

where the $\chi$-integration runs from $-i\infty$ to $i\infty$. See Eq. (4) of the supplement [16] for more detail on the derivation of this equation. Employing the slowness of the $\chi(t)$ field, the Gaussian integral over the fast $y(t)$ can be evaluated using the Fourier transformation. This leads to an effective Lagrangian for $\chi$ in the form

$$\mathcal{L}_\chi = \int \frac{d\omega}{2\pi}\,\ln\!\left(1 + \frac{4T_y\chi}{\omega^2+4}\right) - \chi y_0^2 = \sqrt{T_y\chi + 1} - 1 - \chi y_0^2. \tag{6}$$

Finally, the $\chi$-integration can be evaluated in the saddle point approximation: $\chi(t) = T_y/4y_0^4 - T_y^{-1}$. This yields the probability of $y$-motion conditioned on $\langle y^2\rangle = y_0^2(t)$:

$$P[y_0] \propto e^{-\int dt\, E_y(y_0)}, \qquad E_y(y_0) = \frac{T_y}{4y_0^2} - 1 + \frac{y_0^2}{T_y}\,. \tag{7}$$

Notice that $E_y$ is non-negative and equal to zero if and only if $y_0^2 = T_y/2$. Therefore, the condition $y_0^2(\pm\infty) = T_y/2$ is necessary for convergence of the integral in Eq. (7). The saddle point calculation is justified as long as $\int dt\, E_y[y_0(t)] \gg 1$. A more detailed calculation of Eqs. (5)-(7) is found in the supplementary material [16].

Having found the conditional probability of $y$-motion with a given profile of $\langle y^2\rangle$, we turn now to the $x$-degree of freedom. According to the scale separation assumption, it is governed by the Langevin equation $\dot{x} = x^2 - y_0^2(t) + \xi_x(t)$, where $y_0^2(t)$ is a slow function of time with $y_0^2(\pm\infty) = T_y/2$ and $y_0^2(0) < T_y/2$. Our goal is to evaluate the escape rate of the $x$-variable from its metastable minimum at $x = -\sqrt{T_y/2}$ during the time when $y_0^2(t)$ is suppressed with respect to its asymptotic values. We then maximize this escape rate, taken with weight $P[y_0]$, Eq. (7), against the optimal time-dependent variance $y_0(t)$.

Since the escape rate in the $x$-direction is expected to be small, it can be found through an eikonal treatment of the corresponding FP equation [17]. The proper FP Hamiltonian has the form

$$\mathcal{H}[x, p_x; y_0(t)] = p_x[-V'(x) - y_0^2 + T_x p_x] - E_y[y_0(t)]\,, \tag{8}$$

where $x$ and $p_x$ are canonically conjugate variables, and $y_0(t)$ is an external time-dependent parameter. The last term accounts for the statistical weight of a realization of $y_0(t)$, given by $P[y_0]$, Eq. (7). If $y_0(t)$ is an adiabatically slow function (compared to the time scale of the fast $y$-fluctuations), the escape proceeds along the zero-energy trajectory of this Hamiltonian, which connects the two fixed points $(-\sqrt{T_y/2}, 0)$ and $(+\sqrt{T_y/2}, 0)$ on its $(x, p_x)$ phase plane, Fig. 3. Putting $V(x) = -x^3/3$, one finds for the (slowly varying in time) optimal trajectory

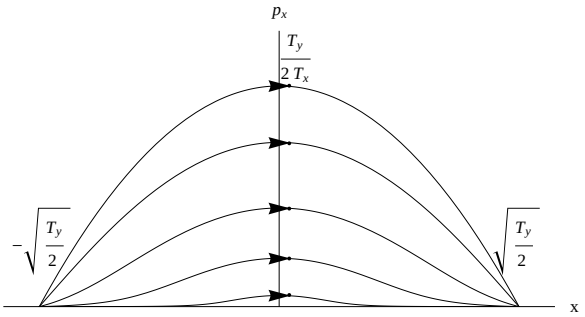


FIG. 3. Phase portrait of the optimal escape paths for different $T_x$. Lower lines correspond to lower values of $T_x$. The momentum has been rescaled by $T_y/T_x$ so that all paths would coincide if they followed simple activation [assumed by Eq. (4)].

$$p_x(x; y_0) = \frac{1}{2T_x}\left[y_0^2 - x^2 + \sqrt{(y_0^2 - x^2)^2 + 4T_x E_y(y_0)}\right]. \tag{9}$$

The corresponding escape time, within exponential accuracy, is given by the classical action, i.e. the area of the phase plane under the zero-energy trajectory

$$\ln t_{\rm esc}[y_0] = S[y_0] = \int_{-\sqrt{T_y/2}}^{\sqrt{T_y/2}} p_x(x; y_0)\, dx. \tag{10}$$

The final step is to find the optimal $y_0$ realization. This is achieved by demanding $\delta S[y_0]/\delta y_0 = 0$, solving for an implicit function of time $y_0 = y_0(x)$ and substituting it back into Eq. (10). This leads to the optimal action, $S_{\rm opt}$, and corresponding escape time $\ln t_{\rm esc} = S_{\rm opt}$. In Fig. 4 this escape time is compared with our Monte-Carlo simulations results, and an excellent agreement is observed.

It is easy to show that, for $T_y \ll \sqrt{T_x}$, the optimal $y_0$ tends to $\sqrt{T_y/2}$ and thus $E_y \to 0$, while $S_{\rm opt} = \sqrt{2}\,T_y^{3/2}/3T_x$. We thus recover Eq. (4). In the opposite limit $T_y \gg \sqrt{T_x}$, one finds $y_0(0) \ll \sqrt{T_y/2}$. One can thus simplify Eq. (7) as $E_y \approx T_y/4y_0^2$. With this substitution Eq. (9) can be simplified by the rescaling $x = \tilde{x}(T_xT_y)^{1/6}$ and $y_0 = \tilde{y}_0(T_xT_y)^{1/6}$, which brings the action (10) into the form $S = \sqrt{T_y/T_x}\int \tilde{p}(\tilde{x}; \tilde{y}_0)d\tilde{x}$. The integration limits are $\pm(T_y^2/T_x)^{1/6} \to \pm\infty$ in the limit of interest, while $\tilde{p} = \left[\tilde{y}_0^2 - \tilde{x}^2 + \sqrt{(\tilde{y}_0^2 - \tilde{x}^2)^2 + \tilde{y}_0^{-2}}\right]/2$ is a parameterless function. Optimizing it over $\tilde{y}_0$ and

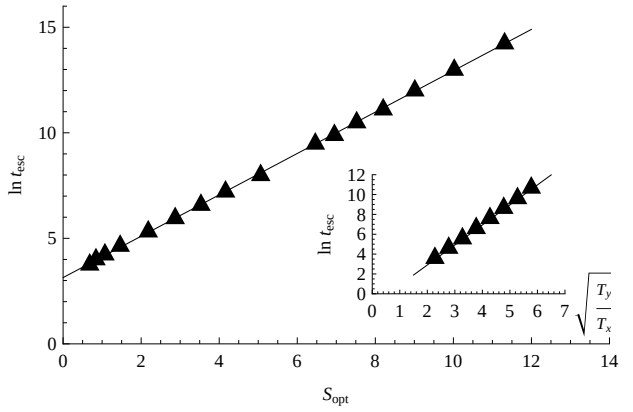


FIG. 4. Simulated escape times vs. the optimal action for $T_y = 0.05$ and varying $T_x$ ($\epsilon = 0$). Inset: the limit $(T_y^2/T_x)^{1/6} \gg 1$ (with $T_y = 1000$). The straight line is Eq. (11).

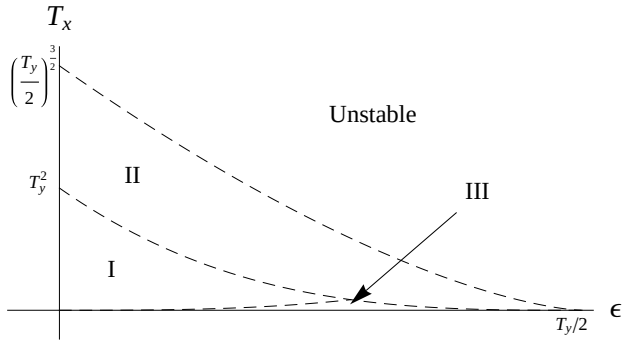


FIG. 5. Phase diagram of the system as a function of $T_x$ and $\epsilon$ with $T_y$ held constant. The dashed lines represent crossovers between different scaling relations. In region I, $\ln t_{\rm esc} = 2\pi/3\sqrt{T_y/T_x}$. In region II, $\ln t_{\rm esc} = 4\,(T_y/2-\epsilon)^{3/2}/3T_x$. In region III, $\ln t_{\rm esc} = \pi T_y/2\epsilon^{3/2}$.

performing $\tilde{x}$-integration, one finds

$$\ln t_{\rm esc} = \frac{2\pi}{3}\sqrt{\frac{T_y}{T_x}}\,, \qquad \sqrt{T_x} \ll T_y\,, \qquad (11)$$

which confirms our qualitative estimates below Eq. (4) and provides the numerical factor. The latter is compared with our Monte-Carlo simulations in the inset of Fig. 4. Notice that the actual condition for the applicability of the asymptotic result (11) is $1 \ll (T_y^2/T_x)^{1/6}$. Again, the population lifetime *increases* with the $y$-noise strength. Notice also that the normal Arrhenius scaling in the parameter $T_x$ gives way to a stretched exponential law with ${T_x}^{-1/2}$. A similar transition is known as Efros-Shklovskii law [18] in the context of hopping transport in disordered semiconductors.

We consider now deviations from the bifurcation point, i.e. $\epsilon \neq 0$. If $|\epsilon| \gg T_y$, the deterministic "force", cf. Eq. (2), is very strong, and the $y$-noise does not affect the system's persistence time. At $\epsilon = \epsilon_c = T_y/2$ the effective force associated with the $y$-noise is canceled by the deterministic $\epsilon$-force. This causes a noise-induced shift in the bifurcation of the $x$-dynamics. That is, it is much harder to destabilize the population in the presence of strong $y$ noise. In the vicinity of this noise-shifted bifurcation one finds the standard scaling of the lifetime $\ln t_{\rm esc} = 4\,(\epsilon_c - \epsilon)^{3/2}/3T_x$, cf. Eq (4).

On the other hand, away from the the noise-shifted bifurcation, i.e. at $|\epsilon - \epsilon_c|/\epsilon_c > (\sqrt{T_x}/T_y)^{2/3}$, the scaling changes qualitatively. To find the new scaling we look for the zero energy trajectory of the Hamiltonian (8) with $\epsilon \neq 0$ and $E_y = T_y/4y_0^2$ and optimize the action over $y_0(x)$, as explained above. In this way we find

$$\ln t_{\rm esc} = \frac{2\pi}{3}\sqrt{\frac{T_y}{T_x}}\;\; \mathcal{S}\left[\frac{\epsilon}{(T_xT_y)^{1/3}}\right], \quad \sqrt{T_x} \ll T_y\,, \quad (12)$$

where the universal function $\mathcal{S}(\tilde{\epsilon})$ has the following asymptotic limits: $\mathcal{S}(\tilde{\epsilon}) \approx 1 - 0.71\tilde{\epsilon}$ for $\tilde{\epsilon} \ll 1$ and $\mathcal{S}(\tilde{\epsilon}) \approx 3\;\tilde{\epsilon}^{-3/2}/4$ for $\tilde{\epsilon} \gg 1$. This means that the scaling of the population lifetime given by Eq. (11) is basically intact as long as $\epsilon \lesssim (T_xT_y)^{1/3}$. In the opposite limit, the escape time scales as

$$\ln t_{\rm esc} = \pi T_y/2\epsilon^{3/2}. \qquad (13)$$

This is independent of $T_x$. For $\epsilon > (T_xT_y)^{1/3}$ the system can escape even at $T_x = 0$ via paths with unusually small $y$. Figure 5 shows the regions where the three scaling relations (4), (11), (13) are valid. More detailed results for $\epsilon \neq 0$ are presented in the supplementary material.

We have focused on the limit where $T_x \ll T_y$. In this regime, the system typically remains in the vortex for many revolutions before ultimately escaping. There is then a time scale separation between the fast $y$-motion and the slow $x$-dynamics. In the opposite limit, this separation no longer exists. However, the system is not trapped by $y$-fluctuations in this case and is unstable unless confined on the mean-field level ($(-\epsilon)^{3/2} \gg T_x$).

In summary, we have studied a novel system where strong noise creates metastability. Increasing the noise strength $T_y$ increases the lifetime of the (vortex-like) metastable state. Escape from this state is governed by a variety of scaling relations depending on the relative role of $T_x$ (the strength of noise in the total population size) and $T_y$ (the strength of noise in the differential size).

We are grateful to J. Krug and M. Dykman for valuable discussions. This research was supported by NSF Grant DMR-0804266 and U.S.-Israel Binational Science Foundation Grant 2008075.

[1] I. Dayan, M. Gitterman, and G.H. Weiss, Phys. Rev. A **46**, 757 (1992).

[2] R.N. Mantegna and B. Spagnolo, Phys. Rev. Lett. **76**, 563 (1996); A. Fiasconaro and B. Spagnolo, Phys. Rev. E **80**, 041110 (2009).

[3] A. Mielke, Phys. Rev. Lett. **84**, 818 (2000).

[4] V. Guttal and C. Jayaprakash, Ecol. Modell. **201**, 420 (2007).

[5] P. D'Odorico, F. Laio, and L. Ridolfi, Proc. Natl. Acad. Sci. USA **102**, 10819 (2005).

[6] R. Ibrahim, J. Vib. Control **12**, 1093 (2006).

[7] R. Abta, M. Schiffer, and N.M. Shnerb, Phys. Rev. Lett. **98**, 98104 (2007).

[8] M. Assaf and B. Meerson, Phys. Rev. Lett. **100**, 58105 (2008).

[9] J. Atalaya, A. Isacsson, and M. Dykman, Phys. Rev. Lett. **106**, 227202 (2011).

[10] P. Moran, *The Statistical Processes of Evolutionary Theory* (Clarendon Press, Oxford, 1962).

[11] N. van Kampen, *Stochastic Processes in Physics and Chemistry* (North Holland, Amsterdam, 1992).

[12] B. Sun, J. Lin, E. Darby, A.Y. Grosberg, and D.G. Grier, Phys. Rev. E **80**, 010401(R) (2009).

[13] P. Martin, E. Siggia, and H. Rose, Phys. Rev. A **8**, 423 (1973).

[14] C. de Dominicis, J. Physique (Paris) **37**, 1 (1976).

[15] H. Janssen, Z. Physik B. **23**, 377 (1976).

[16] On-line supplementary material.

[17] M. Freidlin and A. Wentzell, *Random Perturbations of Dynamical Systems* (Springer-Verlag, Berlin, 1984); M. Dykman and M. Krivoglaz, "Physics Reviews", **5**, 266 (1984); R. Graham, *in "Theory of Continuous Fokker–Planck Systems"*, edited by F. Moss and P. McClintock (Cambridge University Press, Cambridge, 1989) Chap. 7, p. 225.

[18] B. Shklovskii and A. Efros, *Electronic Properties of Doped Semiconductors*, Vol. 1 (Springer-Verlag, Berlin, 1984).